Optimization Approaches for Soft–Tissue Prediction in Craniofacial Surgery Simulation

Matthias Teschner, Sabine Girod, and Bernd Girod

University of Erlangen-Nuremberg
Telecommunications Laboratory
Cauerstr. 7, D-91058 Erlangen, Germany
Phone: +49-9131-8528904, Fax: +49-9131-8528849
teschner@nt.e-technik.uni-erlangen.de
http://www-nt.e-technik.uni-erlangen.de/~teschner/

Abstract. A system for interactive, 3–D, craniofacial surgery simulation is presented. It is used for the 3–D simulation of osteotomies of the facial and skull bones and for the prediction of soft–tissue changes caused by bone movement. The result of the simulation process is a 3–D, photorealistic model of the patient's postoperative appearance that can be viewed from any position.

The system is based on the individual preoperative bone structure of a patient's skull derived from a computer tomography scan and on the patient's photorealistic, preoperative appearance obtained by a laser scanner. The elasto–mechanical properties of the multi–layer soft–tissue are represented by springs. The model incorporates additional features such as skin turgor, gravity, and sliding bone contact.

The prediction of soft–tissue deformation due to simulated bone movement is computed using an optimization approach. Several optimization methods have been tested and compared with regard to robustness of the simulation result and to computational costs.

While the osteotomy simulation can be performed interactively, the computation of the corresponding soft–tissue changes usually takes less than 10 seconds even in sophisticated cases. Tests have been performed on a SGI O2 R10000, 175MHz. The system is able to simulate bimaxillary osteotomies, physiological jaw movement and has been used in the planning process in case of a craniosynostosis.

1 Introduction

The success of complex craniofacial surgical procedures is critically dependent on careful planning. The planning process is aimed at the restoration of functionality and at the improvement of the patient's aesthetics. There are two principal methods of planning surgeries based on models. One method is to build physical models that are generated from CT scans, e. g., stereolithography. These realistic models improve osteotomy planning and allow accurate manufacturing of

C. Taylor, A. Colchester (Eds.): MICCAI'99, LNCS 1679, pp. 1183–1190, 1999.

transplants. Moreover, these models can be used for educational purposes and demonstrations. While physical models provide information on the bone structure, they do not contain knowledge of the soft–tissue, which is of importance to assess the patient's aestethics. The second method of planning craniofacial surgical procedures is to utilize medical imaging for generating computer models [1,2,3,4,5,6,7]. Computer models are more flexible than physical models and are able to provide more information by integrating several modalities. A multimodal computer model of the bone structure and soft–tissue can be used for simulating osteotomies as well as for assessing the patient's appearance. Various simulations can be performed with less additional effort compared to physical models. This is especially helpful in cases where various surgical options are possible.

In our laboratory, we have investigated methods for craniofacial surgery simulation based on 3–D computer models since 1993 [8,9]. In this paper, a refined system is presented, that uses an optimization approach for fast soft–tissue simulation. The paper is organized as follows. In the next section the generation of the 3–D computer models of the bone structure and the face surface is described. In Section 3 the structure and parametrization of the soft–tissue model is described. In Section 4 optimization methods are compared that are used to estimate the soft–tissue deformation due to bone realignment. Simulation results are presented in Section 5.

2 Data Acquisition

Triangle meshes that describe the surface of the face and the bone structure of the head are the basic elements of the simulation process. These meshes are built using two different sensory modalities. A CT scan provides the anatomically correct representation of the bone structure and a laser scanner records a photorealistic, 3–D model of the patient's face. The triangle mesh that represents the surface of the bone structure is generated by segmenting bone from the CT scan and applying the Marching–Cubes–algorithm [10] to the result. An implementation of these methods is adopted from [6]. The triangle mesh that represents the face surface is computed from the depth and color map of the laser scan.

Both modalities are registered by exploiting corresponding cephalometric landmarks of the laser scan and the skin surface taken from the CT scan [6].

3 Soft–Tissue Model

Given the triangle meshes that represent the skull and the face, the soft–tissue model is generated. In recent years, several soft–tissue models based on springs or finite elements have been developed [3,5,6,11,12], [13]. As computational costs for finite–element methods are high and these methods seem to be less suitable for interactive applications, in our work, a mesh of springs is utilized. The springs are categorized according to their location and function (Fig. 1):

– *Layer springs* represent soft–tissue layers. In order to model differentiated elasto–mechanical properties of soft–tissue layers, each layer is represented by a particular class of springs. The number and the thickness of soft–tissue layers are variable. Simulations have been performed with one, three, and five layers.
– *Bone springs* represent connections between bone and soft–tissue. Only some regions of the soft–tissue are connected to the underlying bone structure. To mimic sliding contact, these connections are modeled using springs.
– *Boundary springs* prevent the soft–tissue model from undergoing global transformation. Due to the fact that the face model does not include the complete head surface but only the facial region, these springs anchor the face and the underlying soft–tissue in space.

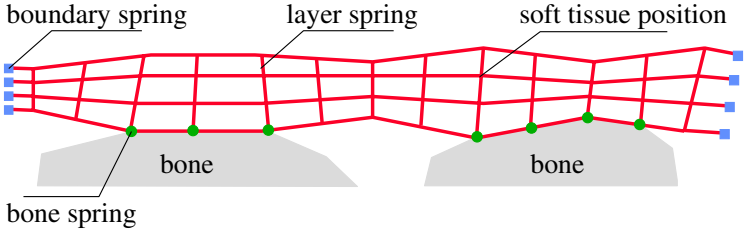

Fig. 1. Soft tissue model.

A spring is characterized by a spring constant k, which describes its stiffness, and by a length l. Every spring class is parametrized with a particular spring constant to model the elasto–mechanical properties of the corresponding soft–tissue layer. Bone springs and boundary springs are parametrized with a comparatively large spring constant. The length of bone springs and boundary springs is zero. The springs that represent the skin surface are given a certain strain. This strain corresponds to the skin turgor. Setting the natural length of all surface springs to $c_{turgor} \cdot l$, with $0 < c_{turgor} < 1$, introduces a certain strain. The difference of l and $c_{turgor} \cdot l$ corresponds to the desired skin turgor.

A *soft–tissue position* is characterized by a location $P \in \mathbb{R}^3$ and a mass m in order to enable simulation of gravity. Every soft–tissue layer is parametrized by an overall mass, which is distributed according to the topology of the representing soft–tissue positions.

Due to the masses and the strain of the surface there are forces at each soft–tissue position. In order to prevent the model from changing without performing any bone realignment and obtaining a stable equilibrium of the mesh, the sum of these forces has to be zero. This is achieved by determining appropriate strains for all springs, given the strain of the skin surface.

4 Soft–Tissue Deformation

The described soft–tissue model is used to estimate soft–tissue deformation due to simulated bone realignment. Basically, the soft–tissue deformation is computed by applying an optimization method that minimizes the energy of the spring mesh. In the initial state of the simulation process the energy is zero. The energy is increased by performing bone transformation. An optimization process deforms the spring mesh in order to minimize the energy. The energy function

$$f(P_0, P_1, \ldots, P_{N-1}) = \lambda \sum_i k_i (l_{0i} - l_i)^2 + (1 - \lambda) \sum_j (v_{0j} - v_j)^2 \qquad (1)$$

depends on $3 \cdot N$ independent variables determining N soft–tissue positions $P_i \in \mathbb{R}^3$. It mainly captures differences between initial spring lengths l_{0i} and current spring lengths l_i and differences between initial volumes v_{0i} and current volumes v_i. The values k_i are spring constants, and λ $(0 < \lambda < 1)$ weights the influence of both terms of the function. The values v_i and v_{0i} are volumes of basic elements of the soft–tissue. The volume consists of prisms.

The initial state of the mesh is characterized by $l_i = l_{0i}$ for every spring. Bone movement leads to $l_i \neq l_{0i}$ and $(l_{0i} - l_i)^2 > 0$ for certain bone springs and to $f(P_0, P_1, \ldots, P_{N-1}) > 0$. Now, new soft–tissue positions P^* are computed by minimizing f. These values P^* describe the deformed soft–tissue:

$$P_0^*, P_1^*, \ldots, P_{N-1}^* = \operatorname{argmin} f(P_0, P_1, \ldots, P_{N-1}). \qquad (2)$$

During the minimization process there are no additional restrictions applied to the soft–tissue positions P apart from the energy function. All soft–tissue positions are considered in the minimization process, regardless of the simulated bone realignment.

Four optimization methods have been compared with regard to computational costs and robustness of the result (Tab. 1). All optimization methods are iterative processes. They terminate if the difference of two P^* or the difference of two evaluations of f in successive steps is tolerably small. This tolerance can be chosen. On one hand, it influences the accuracy of the minimum, on the other hand it has an effect on the computation time. The slightly different minima found by the optimization algorithms (Tab. 1) are due to this tolerance. Some methods require the calculation of partial derivatives. The methods differ in the amount of allocated memory. The order of additional memory that is needed by an optimization method is important due to the fact that its amount is dependent on the number of soft–tissue positions. If the model consists of 3000 positions, then the energy function (1) has 9000 parameters and an optimization method that requires memory in order of N^2 would need a multiple of $81MByte$ memory instead of a multiple of $9kByte$ for an algorithm with order of N. All optimization methods are described in [14].

Tests have shown that the conjugate gradient method provides reliable results and is very efficient with regard to memory and computational complexity.

Optimization method	Order of additional memory	Requires partial derivatives	Time $[s]$	min f
Conjugate gradient, parabolic interpolation	N	yes	0.60	4.33
Conjugate gradient, derivative based	N	yes	2.21	4.33
Direction set (Powell)	N^2	no	81.43	4.33
Variable metric (quasi–Newton)	N^2	yes	2.91	4.30

Table 1. Comparison of optimization methods using a synthetic data set, the energy function (1), and performing an exemplary bone movement. 138 soft–tissue positions P_i, 986 springs, 144 volumes (SGI O2, R10000, 175MHz). N is the number of parameters of the energy function.

Parabolic interpolation is used for 1–D sub–minimization due to the quadratic form of f. Although partial derivatives of the energy function are calculated by this optimization method, its computational expense is comparatively low because of the similarity of the energy function and its partial derivatives. The partial derivatives are responsible for fast convergence of the optimization process and fast convergence reduces the number of function evaluations.

In addition to computational costs another important criterion of an minimization algorithm is the quality of the minimum found. It cannot be guaranteed that the minimum P^* is the global minimum, and it is difficult to prove that fact in a space with $> 10^3$ dimensions. A method to check the robustness of the minimum P^* is to perform a certain bone movement in different ways and to compare the results. If only a small movement is performed, the distance of the initial soft–tissue positions P and P^* is small, f is comparatively small, and the global minimum is likely to be found. For example, translating a bone by 0.1mm ten times or translating a bone by 1mm once should lead to the same P^*. Several tests using the multidimensional conjugate gradient method have been performed and all minima have been reliable.

5 Results

Table 2 and Fig. 2–4 show examples of simulations performed. The soft–tissue prediction is tested with two individual patient data sets. Several simulations of bone movement have been applied to each model. The last column of Tab. 2 shows the maximum time needed by the optimization process. All tests have been performed on a standard workstation SGI O2, R10000, 175MHz. Fig. 5 shows parts of the simulated planning process in case of a craniosynostosis. In this case, only cutting of the bone structure and its realignment has been simulated.

Fig.	Number of soft–tissue positions	Number of springs	Number of volumes	Max. simulation time [s]
2, 3	754	6067	874	1.1
4	2092	16547	2820	3.3

Table 2. Model parameters and simulation speed.

(a) (b) (c) (d) (e)

Fig. 2. Craniofacial surgery simulation for patient 1. a) Preoperative appearance. b) Simulated postoperative appearance. c) Postoperative appearance. d) Preoperative bone structure. e) Simulated postoperative bone structure. The upper jaw is repositioned 4mm forward and 2mm upward anteriorly and 4mm posteriorly. The lower jaw is moved backwards 5mm.

6 Conclusion

In this paper, a new, efficient and robust approach to soft–tissue prediction has been presented. It is based on an optimization method and has been tested with several individual patient data sets. The soft–tissue prediction is integrated in a system for craniofacial surgery simulation. It simulates bimaxillary osteotomies and physiological jaw movement and predicts the soft–tissue changes caused by bone realignment. Ongoing work focuses on the integration of interactive collision detection and collision response algorithms into the system to enable a realistic simulation of bone movement and transplants. As well as estimating the patient's static postoperative appearance and simulating physiological bone movement, the visualization of the patient's post–operative facial expressions is very useful. Therefore, it is planned to add muscles to the existing soft–tissue model. Further, it is intended to register very accurate measurements of the jaws with the CT scan, in order to consider the occlusion of the jaws in the planning process.

(a) (b) (c) (d)

Fig. 3. Simulated physiological lower jaw movement for patient 1.

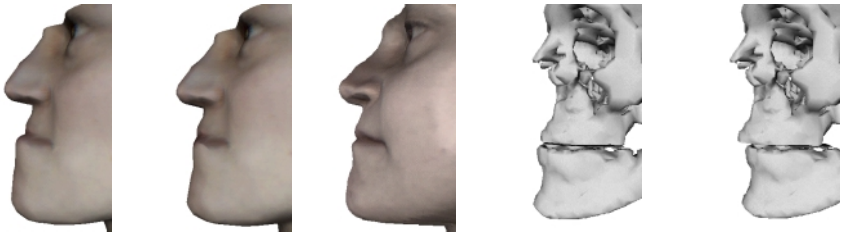

(a) (b) (c) (d) (e)

Fig. 4. Craniofacial surgery simulation for patient 2. a) Preoperative appearance. b) Simulated postoperative appearance. c) Postoperative appearance. d) Preoperative bone structure. e) Simulated postoperative bone structure.

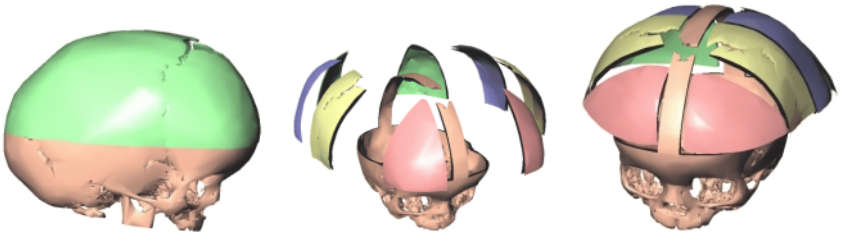

(a) (b) (c)

Fig. 5. Planning process in case of a craniosynostosis. a) Reconstructed preoperative skull. b) Segmentation of the Cranial Vault. c) Reconstruction of the Cranial Vault.

Acknowledgement

This work is supported by the Deutsche Forschungsgemeinschaft DFG (SFB 603, Project C4). Patient data have been provided by the Maxillofacial Surgery Department of the University of Cologne, by the Maxillofacial Surgery Department of the University of Erlangen–Nuremberg, and by the Childrens' Hospital of the University of Erlangen–Nuremberg.

References

1. R. H. Taylor, S. Lavellee, G. C. Burdea, R. Mösges. *"Computer Integrated Surgery – Technology and Clinical Applications"*. MIT Press, Cambridge, Massachusetts, USA, 1996. 1184
2. R. Kikinis, H. Cline, D. Altobelli, M. Halle, W. Lorensen, F. Jolesz. "Interactive Visualization and Manipulation of 3D Reconstructions for the Planning of Surgical Procedures". In *Proceedings of Visualization in Biomedical Computing VBC '92*, pages 559–563, 1992. 1184
3. H. Delingette, G. Subsol, S. Cotin, J. Pignon. "A Craniofacial Surgery Testbed". *Technical Report 2119, Institut National de Recherche en Informatique et Automatique, (France)*, 1994. 1184
4. R. A. Robb, B. M. Cameron. "Virtual Reality Assisted Surgery Program". *Medicine Meets Virtual Reality III: Interactive Technology & the New Paradigm for Healthcare*, January 1995. 1184
5. M. Bro-Nielsen. "Finite Element Modeling in Surgery Simulation". *Proceedings of the IEEE: Special Issue on Virtual & Augmented Reality in Medicine*, 86(3):524–530, March 1998. 1184
6. E. Keeve, S. Girod, R. Kikinis, B. Girod. "Deformable Modeling of Facial Tissue for Craniofacial Surgery Simulation". *Computer Aided Surgery*, 3(5), 1998. 1184
7. P. Bohner, P. Pokrandt, S. Haßfeld. "Simultaneous Planning and Execution in Cranio-Maxillo-Facial Surgery". In *Medicine Meets Virtual Reality 4 (MMVR4)*, 1996. 1184
8. S. Girod, E. Keeve, B. Girod. "Soft Tissue Prediction in Orthognatic Surgery by 3D CT and 3D Laser Scanning". *Journal of Oral and Maxillofacial Surgery Suppl.*, 51:167, 1993. 1184
9. E. Keeve, S. Girod, P. Pfeifle, B. Girod. "Anatomy–Based Facial Tissue Modeling Using the Finite Element Method". In *Proc. IEEE Visualization*, 1996. 1184
10. W. E. Lorensen, H. E. Cline. "Marching Cubes: A High Resolution 3D Surface Construction Algorithm". *SIGGRAPH '87, ACM Computer Graphics*, 21(4):163–169, 1987. 1184
11. W. Maurel, Y. Wu, N. Magnenat Thalmann, D. Thalmann. *"Biomechanical Models for Soft Tissue Simulation"*. Springer, Berlin, Germany, 1998. 1184
12. H. Delingette. "Toward Realistic Soft-Tissue Modeling in Medical Simulation". *Proceedings of the IEEE: Special Issue on Virtual & Augmented Reality in Medicine*, 86(3):524–530, March 1998. 1184
13. R. M. Koch, M. H. Gross, D. F. Bueren, G. Frankhauser, Y. Parish, F. R. Carls. "Simulating Facial Surgery Using Finite Element Models". *SIGGRAPH '96, ACM Computer Graphics*, 30, August 1996. 1184
14. W. Press, S. Teulolsky, W. Vetterling, B. P. Flannery. *"Numerical Recipes in C"*. Cambridge University Press, Cambridge, Massachusetts, USA, 2nd edition, 1992. 1186